Available online at www.sciencedirect.com
SCIENCE DIRECT®
PERGAMON
International Journal of Heat and Mass Transfer 46 (2003) 1545–1552
International Journal of HEAT and MASS TRANSFER
www.elsevier.com/locate/ijhmt

Finite element modeling of the porosity formation in castings

I.H. Katzarov *

Institute of Metal Science, Bulgarian Academy of Sciences 67, Shipchenski prohod str., 1574 Sofia, Bulgaria

Received 9 October 2002

Abstract

The aim of the present paper was to contribute to understanding the origin and effects of porosity in aluminum die-castings by characterizing the distribution and geometry of the porosity. It also seeks to develop a predictive model for microporosity formation during solidification through an analysis of the alloy solidification path, the presence of gas dissolved in the molten metal and the flow of liquid metal through the mushy zone. The finite element method was used for solving porosity formation problem jointly with the problem for heat and mass transfer.

1. Introduction

Porosity is a common feature of metal castings, which may or may not be harmful depending on its location, size, and connectivity. In most cases unsound castings will display diminished mechanical properties, leakage in parts intended for hydraulic applications and may cause unacceptable roughness in machined surfaces. For some applications, small pores within the interior of a part may not interfere with the part's function. In certain cases porosity may be advantageous with respect to the desired weight reduction. Understanding the location and geometry of porosity may thus be critical.

The major sources of porosity in cast parts are the reduction in volume which occurs when a liquid metal solidifies, the presence of gas dissolved in the molten metal, and air trapped within the metal during filling of the mold [1–3].

If the liquid metal fails to feed the shrinkage pores could be formed in the casting. Campbell [4] gave an explanation of the feeding mechanisms during alloy solidification. He suggested that interdendritic feeding is the one, which could to the porosity formation in castings.

With the progress of solidification a thermodynamic potential for development of gas bubbles in the interdendritic space may arise. As the solubility of the solid part is less, part of the gas will be rejected from the growing dendrites into the interdendritic liquid during solidification [3]. If the gas content in the interdendritic liquid is high enough so that its pressure exceeds the sum of the local pressure and the surface tension, gas holes will be formed [2].

Concerning the modeling of porosity formation, Piwonka and Flemings [5] employed the pressure drop formula for a laminar flow in the pipe to predict the pore size. Davies [6], and Moosbrugger and Berry [7] used a similar mathematical model to calculate feeding ranges. In their modeling, the solidus temperature was calculated instead of the actual flow velocity. Prasnna Kumar et al. [8] used the FEM, coupling with several experimentally determined coefficients, to predict the feeding efficiency. Kubo and Pehlke [9] presented a model which includes both shrinkage and gas porosity. Pourier et al. [10] established a thermodynamic model, which was able to predict the formation and the amount of porosity in directionally solidified Al–4.5Cu alloy. In their model both shrinkage and gas porosities are considered.

For the above-discussed models, the fluid flow in the mushy zone either was not actually calculated [6–8] or was calculated but based on highly simplified assumptions [5,10], or was decoupled from energy equation.

Modeling of microporosity requires an accurate description of the pressure at each point in the liquid in the mushy zone of a casting. The pressure varies due to the fluid flow required to feed the solidification shrinkage. A fluid flow calculation is therefore necessary.

* Tel.: +359-2-7142-363; fax: +359-2-703-207.
E-mail address: ivo@ims.bas.bg (I.H. Katzarov).

0017-9310/03/$ - see front matter
PII: S0017-9310(02)00444-1

Because of the complex geometry and the combination of thin and thick parts in castings, the programs based on finite differences method (FDM) [9,11] or control volume methods are encountering with difficulties in the approximation of the boundary geometry and the interpolation of boundary conditions. The FEM method has been very successful in many areas of continuous mechanics, where it is now the principal computational method. It has proved its versatility in the treatment of linear self-adjoint problems over complicated geometry.

The objectives of the present study are the development of mathematical model and computer programs for numerical simulation of the nucleation, distribution, geometry and amount of porosity. The FEM was used to provide a more rigorous numerical solution of the pressure in the mushy zone of a casting and flow velocity during solidification.

2. Mathematical formulation

The model describing the porosity formation includes both shrinkage and gas porosity.

Often porosity defects are observed between secondary dendrite arms and at grain boundaries. These types of porosity are considered to form by gas rejection into the liquid during solidification. This porosity arises because the solubility of the gas is less in solid than in the liquid metal, so that some of the hydrogen is expelled into the interdendritic liquid. If the concentration of gas in the interdendritic liquid rises to a value sufficient to exceed the sum of local pressure within the interdendritic liquid and the excess pressure attributed to the surface tension, then microporosity results.

At first gas porosity nucleates at roots of secondary DAS. The free energy change on formation of porosity is [9]

$$\Delta E = V(P - P_g) + A_1\sigma_{SG} + A_2\sigma_{LG} - A_1\sigma_{SL} \tag{1}$$

where V is the volume of porosity, P_g and P are gas pressure and metal pressure, A_1 and A_2 the areas of solid–gas and liquid–gas interface, and σ_{SG}, σ_{LG} and σ_{SL} are solid–gas, liquid–gas and solid–liquid surface tensions (interface energies). When gas porosity forms at equilibrium ΔE is zero. The first term on the right side represents the free energy change in going from liquid to gas porosity. The other terms represent the free energy change necessary to form the gas porosity surface. In homogeneous nucleation, the first term is required to be a very large negative value to overcome the effect of the gas porosity surface energy. In this case, however, since the effect of surface energy is reduced by the last term, a large negative pressure difference is not required. With the progress of solidification, the gas dissolved in the liquid increases and porosity grows. Since the radius of porosity becomes large enough to decrease the effects of interfacial energy, the porosity can detach from the dendrite. Furthermore at later stage of solidification the neighboring dendrites collide, so that the interdendritic feeding becomes difficult. At that point the porosity is considered to grow to compensate for the solidification shrinkage.

The model describing the shrinkage porosity is based on the pressure drop evaluation in the interdendritic liquid. The local pressure P in the two-phased region is calculated from a system of two differential equations—continuity equation and Darcy law [9].

From a mass balance for a volume element, the continuity equation requires

$$\left(\frac{\rho_S}{\rho_L} - 1\right)\frac{\partial f_L}{\partial t} - \nabla.(f_L\mathbf{u}) + \frac{\partial f_P}{\partial t} = 0 \tag{2}$$

The first term on the left side is the amount of shrinkage, the second term is the amount of liquid input by interdendritic flow. The last term is the amount of porosity growth. The equation indicates that the shrinkage during solidification is compensated by interdendritic flow and the growth of porosity.

From many experiments is known that the interdendritic flow encounters resistance, which is similar to flow in porous medium. The motion equation describing interdendritic flow can be expressed from Darcy's law as

$$\mathbf{u} = -\frac{k}{\nu f_L}(\nabla P + \rho\mathbf{g}) \tag{3}$$

After substituting the velocity of the interdendritic mass feeding, described by the Darcy's law, into the continuity equation the following equation describing the local pressure in the mushy zone is obtained

$$k\Delta P + \nabla k.\nabla P + \rho\nabla k.\mathbf{g} + \mu\left(\frac{\rho_S}{\rho_L} - 1\right)\frac{\partial f_L}{\partial t} + \mu\frac{\partial f_P}{\partial t} = 0 \tag{4}$$

The following boundary conditions are imposed for this equation: along the liquidus isotherm the pressure is equal to the pressure in the molten metal and the liquid metal flows to feed shrinkage

$$u = \left(\frac{\rho_S}{\rho_L} - 1\right)u_L$$

where u_L is the liquid isotherm velocity.

It is necessary to characterize the dendritic structure during solidification in order to assign the permeability for flow of the interdendritic liquid and in order to estimate gas bubble radii.

It is assumed that a gas pore is stable (will not shrink) provided that the supersaturation, or excess pressure, in the gas is sufficiently great to overcome the surface tension when the gas phase has a radius that is small enough to fit in the interdendritic space. The above requirement is expressed as [10]

$$P_g - P = \sigma_{GL}\left(\frac{1}{r_1}+\frac{1}{r_2}\right) \tag{5}$$

where r_1 and r_2 are the principal radii of curvature.

The principal radii of curvature depend upon the volume of the interdendritic space and its geometry and the contact angle at the gas–solid–liquid junction. Since the contact angle is approximately zero the bubble or the bubble cap of the gas phase of minimum excess pressure fits in the local interdendritic space such that $2r_1$ would be equal to the width of the space.

The dimensions of the interdendritic space between the primary dendrite arms are greater than the interdendritic spaces between the secondary dendritic arms; thus less excess pressure would be required for the gas phase existing between the primary than in the secondary. Hence, the primary dendrite arm spacing and the arrangement of the primary dendrite arms are more important than the geometrical properties of the secondary. Based upon dendritic arrangement is shown [10] that the interdendritic space is a groove of width $\delta = f_L d_1/2$. A bubble with minimum excess pressure is one, which fits in the groove and its principal radii of curvature are $r_1 = \delta/2$ and $r_2 = \infty$. Then the minimum excess pressure is

$$P_g - P = \frac{4\sigma_{GL}}{f_L d_1} \tag{6}$$

The primary dendrite arm spacing of an alloy depends on the growth conditions and is expressed in the form

$$d_1 = AG_L^a R^b \tag{7}$$

where G_L is the thermal gradient in front of the dendrites, R is the solidification rate and A, a, b are constants, which can be determined empirically.

The permeability k_0 is calculated from the liquid fraction f_L and dendrite cell size d following Blake–Kozeney equation

$$k_0 = \frac{f_L^3 d^2}{180(1-f_L)^2} \tag{8}$$

The gas pressure is calculated from Eq. (6) assuming the diameter of porosity first being the width of the interdendritic space between the arms of primary

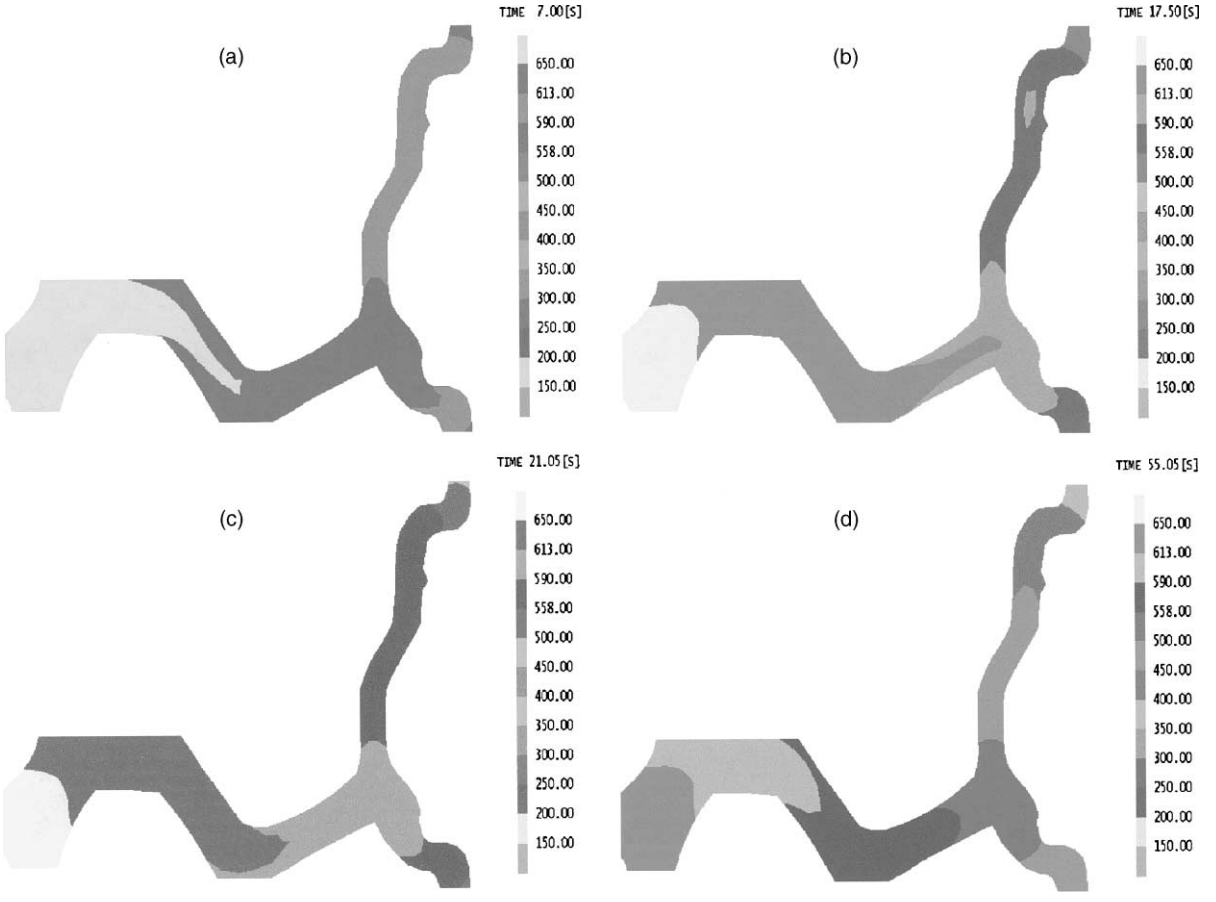

Fig. 1. Calculated evolution of the temperature field (°C) during cooling and solidification of a car wheel.

dendrites. A new amount of porosity is calculated from the conservation equation for gas content. Assuming complete equilibrium, the conservation equation for gas content is

$$[H_0] = (1 - f_L)[H_S] + f_L[H_L] + \alpha\frac{P_g f_P}{T} \tag{9}$$

The left side is the initial hydrogen content $[H_0]$. The first, second and the third terms on the right are the amounts of hydrogen in the solid $[H_S]$, liquid $[H_L]$ and porosity fraction f_P. The Sievert's law for diatomic gas expresses the hydrogen content in the solid and liquid

$$[H_S] = K_{SH}\sqrt{P_g}; \qquad [H_L] = K_{LH}\sqrt{P_g} \tag{10}$$

The porosity problem is solved jointly with the problem for heat and mass transfer. The heat balance equation is expressed as

$$\rho c\frac{\partial T}{\partial t} + f_L\rho c\mathbf{u}.\nabla T = \lambda\Delta T - \rho L\frac{\partial f_L}{\partial t} \tag{11}$$

where $\rho = f_L\rho_L + f_S\rho_S$ is the average density of liquid and solid, ρ_L and ρ_S are the densities for the fully liquid and solid regions, respectively. Here $u(t, \mathbf{x})$ is the velocity of the interdendritic flow, c is the heat capacity, λ is the heat conductivity and L is the latent heat of crystallization. The temperature gradients are small in the mushy zone and the liquid fraction is relatively small, and therefore, the temperature terms for interdendritic flow can be neglected.

To solve this equation the relationship between the liquid fraction and temperature is needed. Using the Scheil model of solidification (complete mixing in the liquid, no diffusion in the solid), the liquid fraction is expressed as

$$f_L = \left(\frac{T - T_m}{T_L - T_m}\right)^{1/(k_0-1)} \tag{12}$$

where T_m is the melting temperature of the pure element, equilibrium segregation coefficient $k_0 = C_S/C_L$.

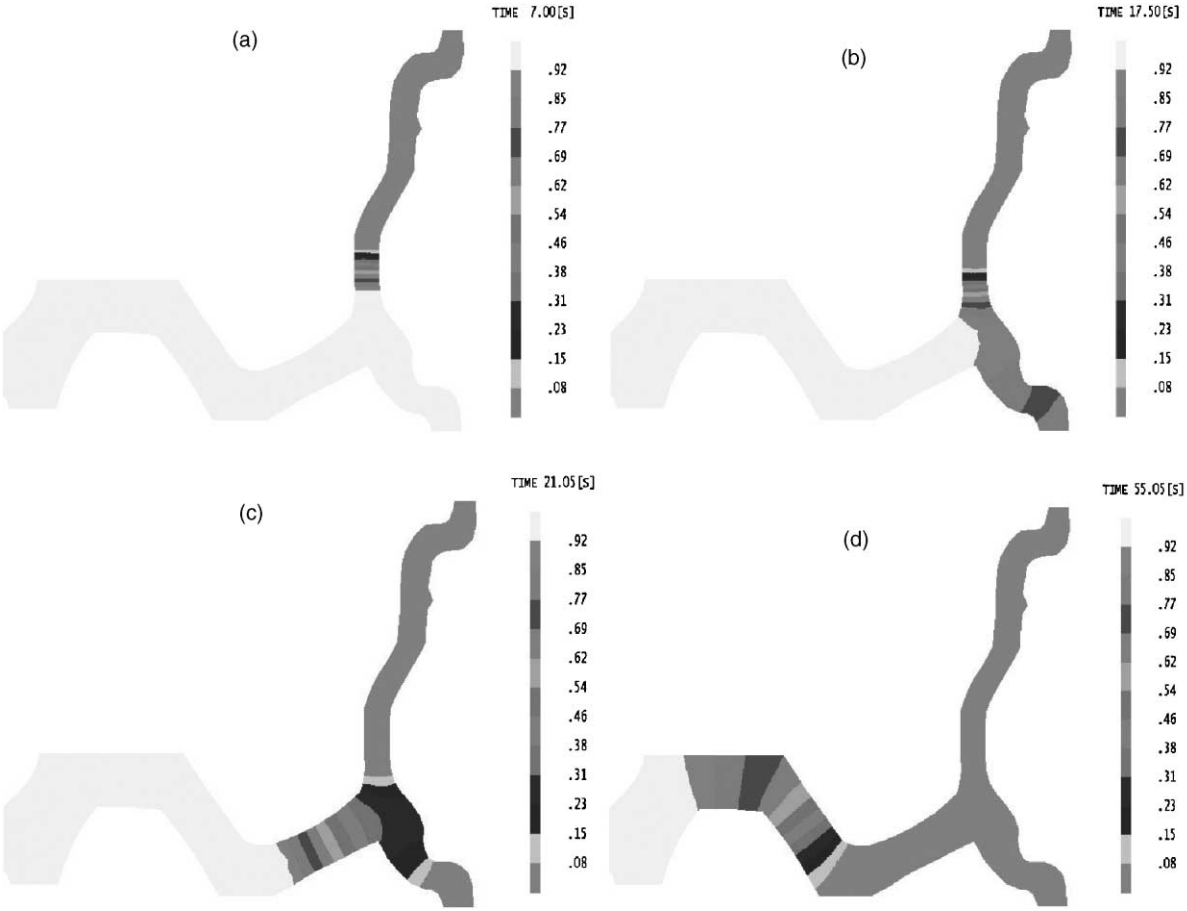

Fig. 2. Calculated evolution of metal pressure (bar) distribution in the mushy zone during solidification of a car wheel for differential pressure of 1 bar.

3. FEM formulation of the interdendritic flow problem

The finite element approximation is based on the weak form of the equation describing the pressure field in the mushy zone, which may be written as [12,13]

$$\int_V \phi\left[k\Delta P + \nabla k.\nabla P + \rho\nabla k.\mathbf{g} + \mu\left(\frac{\rho_S}{\rho_L} - 1\right)\frac{\partial f_L}{\partial t} + \mu\frac{\partial f_P}{\partial t}\right] dV = 0 \quad (13)$$

where V is the volume of the mushy zone of casting. The function ϕ is required to be measurable in Sobolev sense.

From a computational viewpoint a more useful weak form is the Galerkin form, which is derived from the above by the use of Stock's theorem. This form requires minimum continuity of the solutions P.

$$\int_V k\nabla\phi.\nabla P\,dv - \int_S \phi k\nabla P.\mathbf{n}\,d\mathbf{s} - \int_V \phi\left[\rho\nabla k.\mathbf{g} + \mu\left(\frac{\rho_S}{\rho_L} - 1\right)\frac{\partial f_L}{\partial t} + \mu\frac{\partial f_P}{\partial t}\right] dv = 0 \quad (14)$$

where the integration in $\mathbf{s}$ is over the boundary S of V and $\mathbf{n}$ is outward normal vector.

The boundary conditions on the surface are incorporated by the replacement of $k\nabla P$ by $k\mathbf{G} - vf_L\mathbf{u}$ (from Darcy's law).

We approximate the region V by a set of finite elements, in particular a set of 8—node elements in the 3-D case, and introduce parametric approximations, which map these elements onto a standard cube. The subdivision of the domain V into a set of finite elements reduces the original problem to one which is finite dimensional and the values of the pressure are calculated only at the nodes of the elements. In terms of basic function expansion the pressure field is taken to be of the form

$$P \cong \widetilde{P} = \sum_{k=1}^{N} \phi^k(\mathbf{x})P_k \quad (15)$$

The derivatives of $\widetilde{P}$ are calculated in the form

$$\frac{\partial\widetilde{P}}{\partial x_j} = \sum_{k=1}^{N} \frac{\partial\phi^k}{\partial x_j}P_k \quad (16)$$

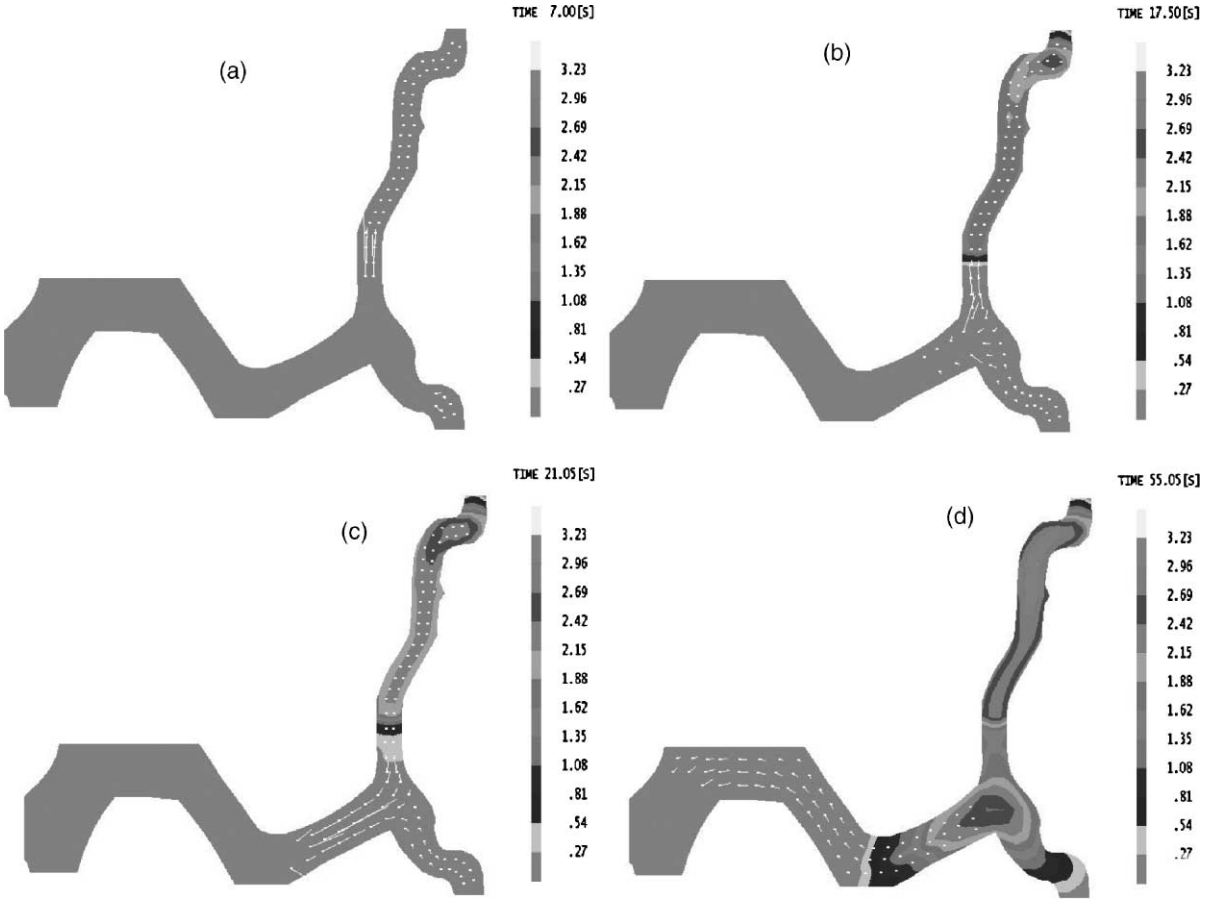

Fig. 3. Calculated evolution of the distribution and amount of porosity (%) and interdendritic flow velocities during solidification of a car wheel for differential pressure of 1 bar.

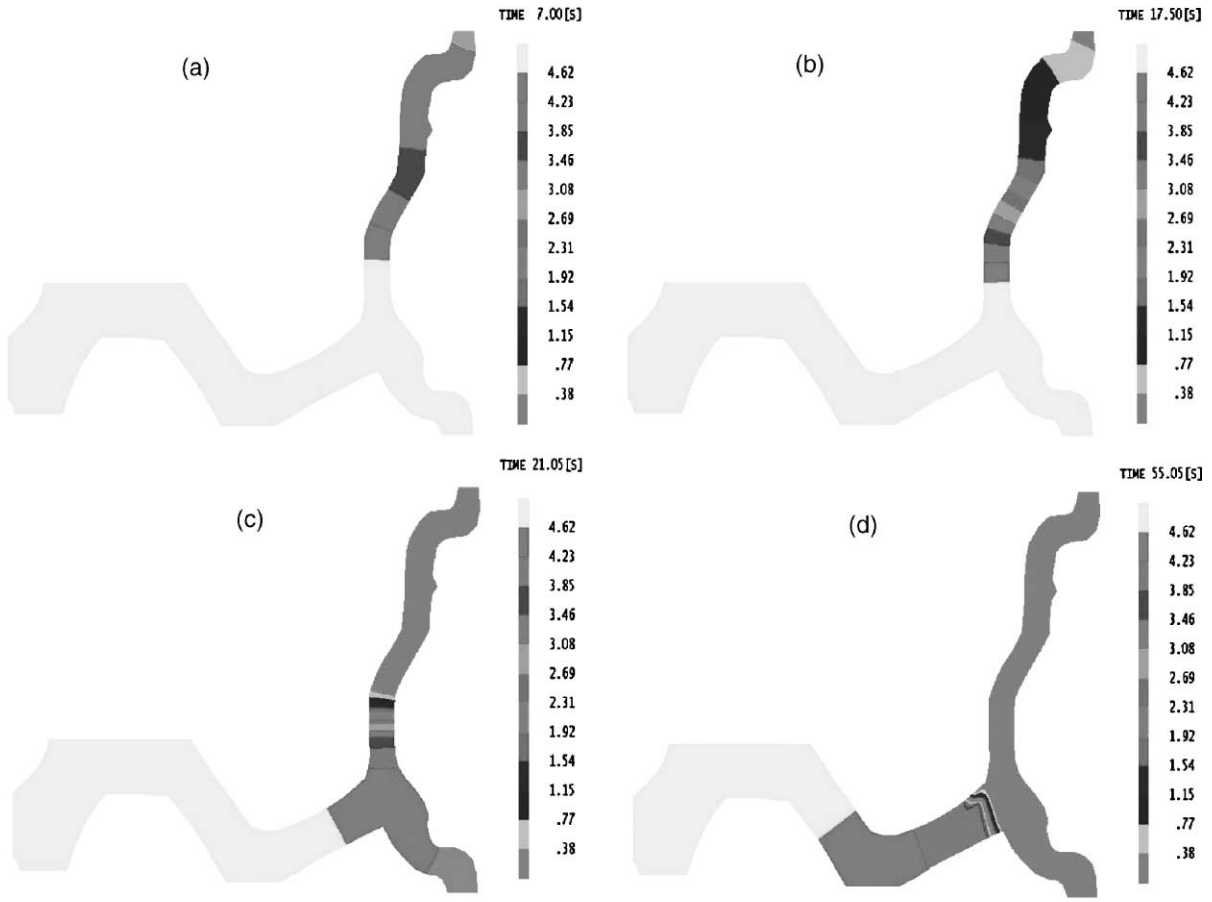

Fig. 4. Calculated evolution of metal pressure (bar) distribution in the mushy zone during solidification of a car wheel for differential pressure of 5 bar.

where N is the number of FE mesh nodes and P_k are the nodal values of P ; ϕ^k are the basic functions, which are assumed to form a complete set of functions over the castings volume. The interpolating functions ϕ^k must be chosen to preserve continuity of pressure between the elements because of the first order derivatives. In this work ϕ^k are chosen to be a set of bilinear pyramid functions

$$\phi^k(p_l) = \delta_l^k = \begin{cases} 1 & k = l \\ 0 & k \neq l \end{cases} \tag{17}$$

The Galerkin approximation satisfies

$$\int_V k\nabla\phi^k.\nabla\widetilde{P}\,\mathrm{d}v + \int_S \phi^k v f_L \mathbf{u}.\mathbf{n}\,\mathrm{d}\mathbf{s} - \int_S \phi^k k\mathbf{G}.\mathbf{n}\,\mathrm{d}\mathbf{s} - \int_V \phi^k \left[\rho\nabla k.\mathbf{g} + \mu\left(\frac{\rho_S}{\rho_L} - 1\right)\frac{\partial f_L}{\partial t} + \mu\frac{\partial f_P}{\partial t}\right]\mathrm{d}v = 0$$

Substituting the derivatives into the Galerkin approximation we obtain a system of linear equations

$$\sum_{l=1}^{N}\left(\int_V k\nabla\phi^k.\nabla\phi^l\,\mathrm{d}v\right)P_l + \int_S \phi^k v f_L \mathbf{u}.\mathbf{n}\,\mathrm{d}\mathbf{s} - \int_S \phi^k k\mathbf{G}.\mathbf{n}\,\mathrm{d}\mathbf{s} - \int_V \phi^k \left[\rho\nabla k.\mathbf{g} + \mu\left(\frac{\rho_S}{\rho_L} - 1\right)\frac{\partial f_L}{\partial t} + \mu\frac{\partial f_P}{\partial t}\right]\mathrm{d}v = 0$$

which can be solved for the unknown nodal values P_k of the pressure field.

4. Results and discussion

Detailed solutions are given for distribution and amount of porosity in car wheel produced by counter pressure casting (CPC) method [14].

First the temperature and change of the solid fraction are calculated from heat balance equation. Finite element method (FEM) based computer program was developed for solving heat transfer and crystallization problem [15]. If the volume element is in the mushy

zone, the variables are calculated in the following manner.

When no porosity has formed, the metal pressure P is calculated from the Eq. (4) describing the local pressure in the mushy zone by FEM, assuming no occurrence of porosity. Then the gas pressure is calculated as the minimum excess pressure required so that the gas bubble is stable Eq. (6), assuming the diameter of porosity being the interdendritic space width. Subsequently, a new amount of porosity is calculated from gas balance equation Eq. (9) and Sievert's law Eq. (10). When the porosity has already formed, the metal and gas pressure are calculated using the amount of porosity before the current time Δt. The procedure described above is repeated over each volume element in the mushy zone and each time step until the required time is reached.

An important parameter influencing on the porosity formation in a CPC unit is the differential pressure applied in the molten metal. We investigated the effect of the pressure, applied in the melt, in two cases—one with differential pressure of 1 bar and the second—with 5 bars.

The solutions include the temperature distribution in casting, the velocity of interdendritic flow, the amount of porosity and pressure drop in casting, shown as graphical output available to users of the computer code

The calculated evolution of the temperature fields and pressure drop in the casting for differential pressure of 1 bar are shown in Figs. 1 and 2. The velocity of the interdendritic flow and the distribution and amount of porosity are presented on Fig. 3. The results of calculations in this case indicate that width of the mushy zone in the rim area is large and the pressure cannot

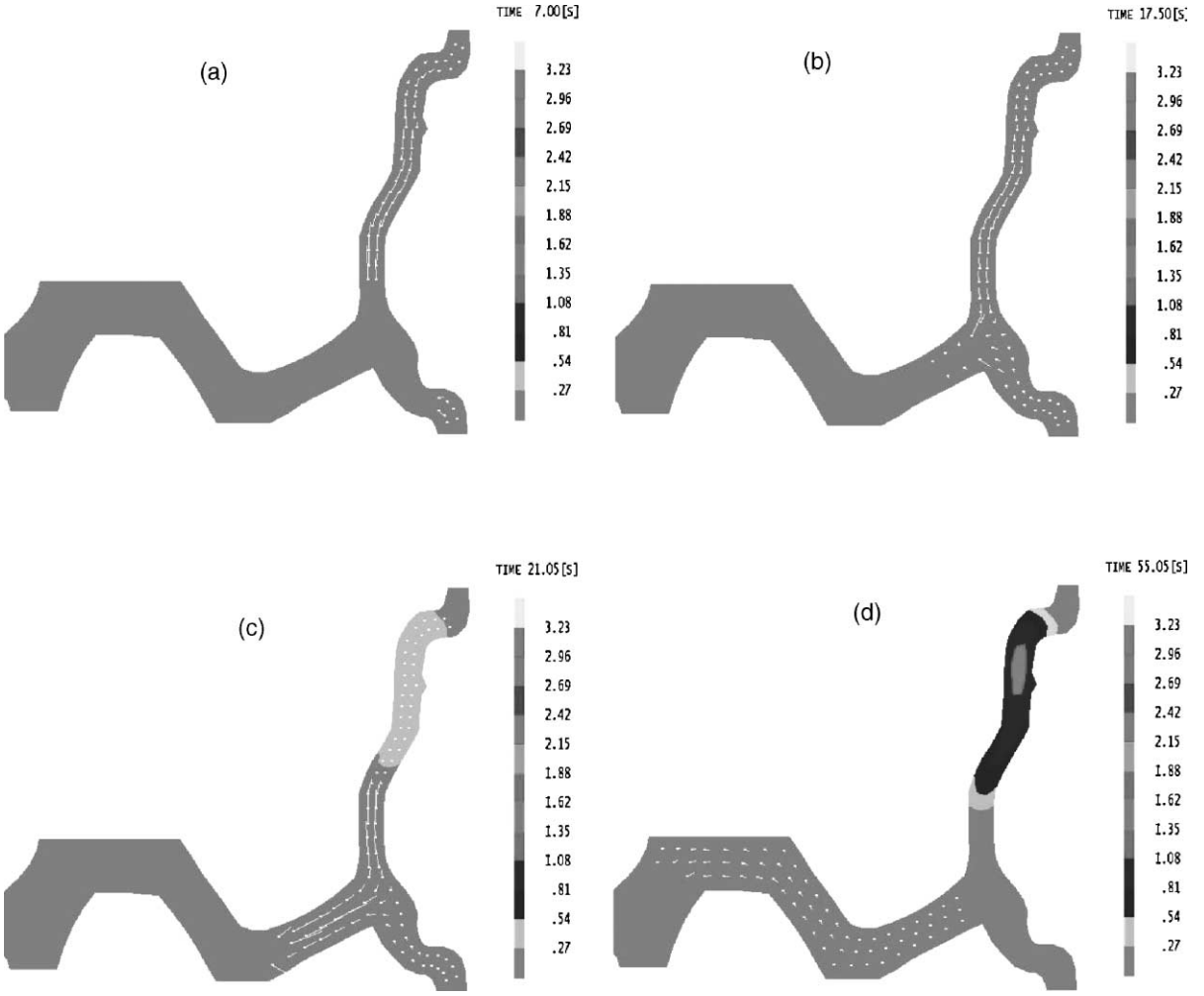

Fig. 5. Calculated evolution of the distribution and amount of porosity (%) and interdendritic flow velocities during solidification of a car wheel for differential pressure of 5 bar.

overcome the resistance to liquid feeding. The pressure in this area drops to zero, the feeding is ceased and the shrinkage during solidification is compensated by porosity growth. Severe porosity defects occur in this case and the volume fraction of porosity exceeds 3%.

The evolution of the pressure field, the interdendritic flow velocity and the distribution and amount of porosity in the mushy zone for differential pressure of 5 bar and for the same cooling conditions are shown in Figs. 4 and 5. In this case the higher pressure, applied in the melt, increases the interdendritic liquid feeding compensating the solidification shrinkage. Hence, the higher interdendritic fluid flow decreases the porosity formation in the casting. The predicted microporosity is consistent with the experimental data.

The present model provides a predictive tool for microporosity formation, which accounts for the detailed effects of alloy solidification behavior without the need for empirical criteria containing numerical parameters, which must be evaluated for each alloy.

Acknowledgements

This work is supported by the National Science Foundation of Bulgaria under contract no. TH-908/1999.

References

[1] G.V. Kutumba Rao, V. Panchanathan, End Chills Influence on Solidification Soundness of Al–Cu–Si Alloy Castings, AFS Cast Metals Res. J. (1973) 135.
[2] M.C. Flemings, Solidification Processing, McGraw-Hill, 1974.
[3] I. Minkoff, Solidification and Cast Structures, John Wiley & Sons, 1986.
[4] J. Campbell, Feeding mechanisms in castings, AFS Cast Metals Res. J. 5 (1) (1969) 1.
[5] T.S. Pivonka, M.C. Flemings, Pore formation in solidification, Trans. Met. Soc. AIME 236 (1966) 1157.
[6] V. Davies, L. de, Feeding range determination by numerical computed heat distribution, AFS Cast Metals Res. J. (1975) 33.
[7] J.C. Moosbrugger, J.T. Berry, Calculation of feeding range data for hypoeutetic A-357 alloy using fem solidification model results, AFS Trans. (1986) 373.
[8] T.S. Prasanna Kumar, S.D. Pathak, O. Prabhakar, Finite element formulations for estimating feeding efficiency factors, AFS Trans. 1 (1985) 789.
[9] K. Kubo, R. Pehlke, Mathematical modelling of porosity formation in solidification, Metall. Trans. B 16B (1985) 359.
[10] D.R. Pourier, K. Yeum, A. Maples, A thermodynamic prediction for microporosity formation in aluminium-rich Al–Cu alloys, Metall. Trans. A 18 (1987) 1979.
[11] I.H. Katzarov, Y.B. Arsov, P. Stoyanov, T. Zeuner, A. Buehrig-Polaczek, P.R. Sahm, Porosity formation in axisymmetric castings produced by counter-pressure casting method, Int. J. Heat Mass Transfer 44 (2001) 111.
[12] O.C. Zienkiewicz, Y.K. Cheung, The finite element method in structural and continuum mechanics, McGraw-Hill, London, UK, 1968.
[13] A.R. Mitchell, R. Wait, The Finite Element Method in Partial Differential Equations, John Willey & Sons, New York, NY, 1977.
[14] A. Balevski, Counter pressure casting, Foundry Trade J. 6 (1989) 746.
[15] I.H. Katzarov, A Finite Element Approach for Simulation of 3D Solidification, J. Mater. Sci. Technol. 10 (4) (2002) 10–16.